DOI: 10.1002/chem.200701520

Interface Engineering of Synthetic Pores: Towards Hypersensitive Biosensors

Federico Mora,[a] Duy-Hien Tran,[a] Natalie Oudry,[b] Gerard Hopfgartner,[b] Damien Jeannerat,[a] Naomi Sakai,[a] and Stefan Matile*[a]

Abstract: Hydrophilic anchoring is introduced as a promising strategy to constructively control the various interactions of synthetic pore sensors with the surrounding biphasic environment. Artificial rigid-rod β barrels are selected as classical synthetic multifunctional pores and random-coil tetralysines are attached as hydrophilic anchors. The synthesis of this advanced pore is accomplished in 32 steps from commercially available starting materials. With regard to pore activity as such, the key impact of hydrophilic anchoring is a change from a Hill coefficient $n<1$ to $n=4$. This change confirms successful suppression of the competing self-assembly with precipitation from the aqueous phase as the origin of the accomplished increase in pore activity. The hydrophilic anchors do not interfere with the blockage of the synthetic pore sensors by anionic analytes. In the case of stoichiometric binding of blockers ($K_D = EC_{50}$ of the pore; EC_{50} = concentration needed to observe 50% pore activity), however, the increase in pore activity achieved by hydrophilic anchoring results in improved pore blockage under high dilution conditions. Controls confirm that this increase does not occur with analytes that do not exhibit stoichiometric binding ($K_D > EC_{50}$). These results not only reveal stoichiometric binding as the expected origin of the sensitivity limit of synthetic pore sensors, they also provide promising solutions for this problem. The combination of hydrophilic anchoring with targeted pore formation emerges as a particularly promising strategy to further reduce effective pore concentrations. The scope and limitations of this approach are exemplified with pertinent analyte pairs that are essential for the sensing of sucrose, lactose, acetate, and glutamate with synthetic pores in samples from the supermarket.

Keywords: ion channels · membranes · peptides · self-assembly · sensors

Introduction

Recently, we obtained experimental evidence[1] for the ability of synthetic ion channels and pores[2–13] to serve as multicomponent sensors[12–24] in samples from the supermarket or the hospital. These findings prompted us to construct refined pore architectures for advanced applications. For multicomponent sensing in complex matrices,[1] synthetic pores are used as general optical transducers of reactions together with enzymes as selective signal generators.[12,13,25] Namely, enzymatic formation or consumption of pore-blocking analytes could be easily monitored as blockage or deblockage of the pore. This response could be used to reliably and rapidly quantify the analytes. Reactive amplifiers have been introduced to covalently capture otherwise elusive analytes after enzymatic signal generation and drag them into the pore for transduction.[1] However, the detection limit of analytes by our pore sensors has so far been consistently in the low micromolar range where the substrate selectivity was also completely lost.[1,25] These phenomena suggested the emergence of stoichiometric binding in this region in which the pore concentration needed to detect activity becomes similar to the dissociation constant K_D of the pore–blocker complex.[26,27] Lowering the effective pore concentration, that is, increasing the activity of the pore as such would thus be the key to increase both sensitivity and selectivity of synthetic pore sensors. In other words, pore–membrane rather than pore–blocker interactions would thus need improvement to reach nanomolar sensitivity.

To address this challenge, we noticed that, ironically, the apparent activity of pores in the membrane often seems to be determined by their solubility in water.[28–31] Namely, hy-

[a] F. Mora, D.-H. Tran, Dr. D. Jeannerat, Dr. N. Sakai, Prof. S. Matile
Department of Organic Chemistry, University of Geneva
Geneva (Switzerland)
Fax: (+41) 22-379-3215
E-mail: stefan.matile@chiorg.unige.ch

[b] N. Oudry, Prof. G. Hopfgartner
School of Pharmaceutical Sciences, University of Geneva
Geneva (Switzerland)

Supporting Information for this article is available on the WWW under http://www.chemeurj.org/ or from the author.

drophilic domains attached to one end of the pore may assure delivery to the vesicle by preventing competing precipitation from the water and enforce vectorial partitioning and transmembrane orientation followed by parallel self-assembly. Exploited to perfection in biology, these various benefits from hydrophilic anchoring are rarely considered in synthetic functional systems.[28–31] Herein, we report hydrophilic anchoring of rigid-rod β-barrel pores, such as **1**, as a promising approach toward multicomponent sensors that can operate at low concentrations with high selectivity (Figure 1).

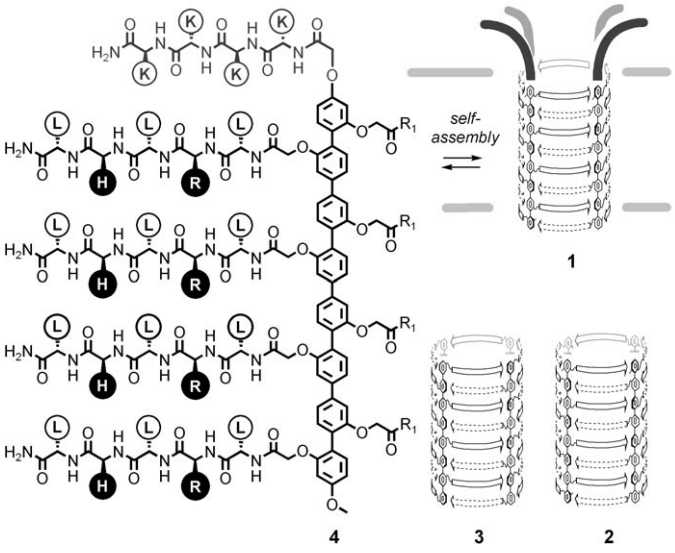

Figure 1. Self-assembly from monomer **4** and the theoretical active structure of pore **1** with hydrophilic anchors together with anchor-free control pores **2** and **3**. β Sheets are shown as gray arrows in the theoretical pore structure, and in the chemical structure, the external amino acid residues are indicated within an empty circle, whereas the internal residues are indicated within a filled circle (the residues are indicated with single-letter abbreviations, see Scheme 2 for full structures).

Results and Discussion

In pore **1**, which is introduced in this report, the rigid-rod β barrel of the classical[32–36] pores **2** and **3** is elongated with four of Tomich's hydrophilic tetralysine (K_4) anchors (Figure 1).[29] Rigid-rod β barrels in general consist of *p*-octiphenyl staves and β-sheet hoops.[32,33] The selected peptide sequence LRLHL produces a hydrophobic outer pore surface (LLL) for contacts with the surrounding bilayer membrane. Functional arginine–histidine (RH) dyads are placed at the inner pore surface to interact with analytes passing by, through the pore, and across the membrane.[12,13,32,33] Except for the NMR tags in position 1^6 and 8^6, the $1^2,2^2,3^3,4^2,5^3,6^2,7^3,8^2$ substitution pattern of the *p*-octiphenyl stave in pore **2** is identical with that in pore **1**.[34] The characteristics of pore **2** and pore **3** with the classical $1^3,2^3,3^2,4^3,5^2,6^3,7^2,8^3$ motif are essentially identical.[34–36]

The cationic K_4 anchors were selected because they were best in an extensive optimization with readily accessible peptidic anion channels.[29] Moreover, cationic anchors were preferred over anionic or neutral anchors because repulsion from the cationic interior of pore **1** was considered as essential to prevent backfolding of the anchor into the pore.

Rigid-rod molecule **4** was envisioned for the parallel self-assembly into transmembrane β-barrel pore **1** with hydrophilic K_4 anchors. This multiple-substituted *p*-octiphenyl **4** was synthesized in 32 steps from commercially available starting materials, including 14 steps of very straightforward peptide synthesis.[37] The key challenge of this synthesis was to attach two different peptide strands to one rigid-rod scaffold. *p*-Octiphenyl **5** with carboxylic acids that carry orthogonal benzyl and *tert*-butyl protecting groups was conceived to address this problem (Scheme 1). The synthesis of this key intermediate **5** by Suzuki coupling of the two differently substituted phenyl termini **6** and **7** to the previously reported *p*-sexiphenyl scaffold **8**[30] appeared not to be problematic.

The K_4-terminal fragment **6** was prepared from resorcinol **9**. Protected as a benzyl ester, one bromoacetate **10** was introduced first by Williamson ether synthesis. Selective *ortho*-iodination of the obtained phenol **11** afforded the aryl iodide **12**. This substrate was needed to introduce the second bromoacetate **13** with the orthogonal *tert*-butyl protecting group. Pinacolboronate **6** was obtained by Pd-catalyzed conversion[38] of aryl iodide **14**.

The other rod terminus **7** was synthesized following recently reported procedures.[39] In brief, *ortho*-iodination of methylresorcinol **15** afforded regioisomer **16** chemoselectively. This reaction was followed by Williamson ether synthesis with *tert*-butyl bromoacetate **13**. The obtained aryl iodide **17** was transformed via boronate **18** to give **7**, which benefits from the increased stability, easier purification, and higher reactivity of the solid potassium trifluoroborates.[40]

The *p*-sexiphenyl **8** was selected as an ideal building block to attach the terminal rod fragments **6** and **7** because of its rapid accessibility from the commercially available biphenyl **19** and *tert*-butyl bromoacetate **13**.[30] In brief, diazide **19** was converted into diiodide **20** and dipinacolboronate **21**. These two monomers were then polymerized under Suzuki coupling conditions. Because of poor solubility, *p*-sexiphenyl **22** could be isolated directly and in good yield from the reaction mixture. Rod **22** was treated with BBr_3 to give oligophenol **23**. This rod **23** was treated with *tert*-butyl bromoacetate **13** to yield the target intermediate **8**. Attachment of fragments **7** to one end of the *p*-sexiphenyl **8** by Suzuki coupling was accomplished following previously reported procedures.[39] The obtained *p*-septiphenyl **24** was subjected to another Suzuki coupling with the K_4-terminal fragment **6**. The product was the desired *p*-octiphenyl scaffold with three different substituents, two of them being chemically differentiated by orthogonal protecting groups.

The NMR spectra of asymmetric oligomers such as **5** can be challenging to fully understand because the presence of several quasi-identical repeats causes extensive signal clustering.[41] However, the recording of high-resolution 2D HSQC and HMBC NMR spectra allowed unambiguous

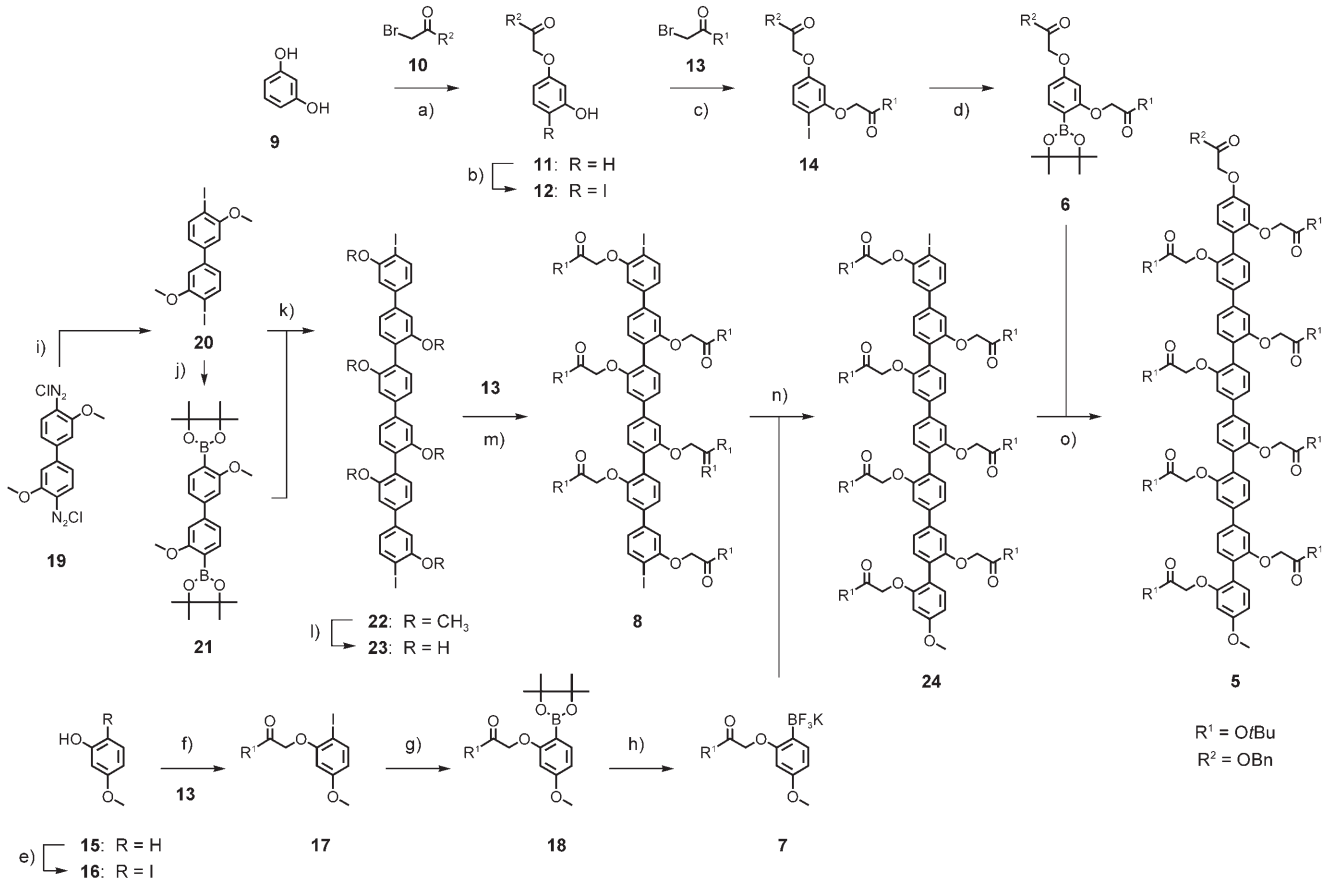

Scheme 1. a) Cs_2CO_3, acetone, 60 °C, 30 min, yield = 75 %; b) I_2, AgOTf, $CHCl_3$, 2.5 h, RT, yield = 40 %; c) Cs_2CO_3, acetone, 65 °C, 30 min, yield = 92 %; d) pinacolborane, [$PdCl_2$(dppf)], Et_3N, CH_3CN, 2 h, 85 °C, yield = 60 %; e–h) see reference [39]; e) AgOTf, I_2, yield = 72 %; f) Cs_2CO_3, yield = 96 %; g) pinacolborane, [$PdCl_2$(dppf)], yield = 88 %; h) KHF_2, quantitative; i–m) see reference [30]; i), KI, yield = 70 %; j) pinacolborane, [$PdCl_2$(dppf)], yield = 69 %; k) [$Pd(PPh_3)_4$], yield = 14 %; l) BBr_3; m) Cs_2CO_3, 92 % (from **22**); n) [$PdCl_2$(dppf)], conversion yield 42 % (from reference [39]); o) [$Pd(PPh_3)_4$], toluene/EtOH 10:1, Na_2CO_3, yield = 80 %. dppf = 1,1′-bis(diphenylphosphanyl)ferrocene.

assignment of all carbon and hydrogen atoms of the key intermediate **5** (see Figure S1 in the Supporting Information).

The Z-protected K_4 anchor **25** was newly prepared in 8 steps by a routine solution-phase peptide synthesis (Scheme 2). The synthesis of the protected LRLHL peptide **26** has been reported previously.[34–36] Chemoselective hydrogenolysis of the terminal benzyl ester of rod **5** liberated the carboxylic acid at one rod terminus without deprotection of those along the rigid-rod scaffold. The deprotected carboxylic acid at one end of rod **27** was coupled with the N terminus of the Z-protected K_4 anchor **25**. The K_4 rod **28** was obtained in good yield. The carboxylic acids along the rigid-rod scaffold **28** were deprotected next with trifluoroacetic acid (TFA). The orthogonal Z protection of the K_4 anchor remained intact in product **29**. The Pmc/Trt-protected (Pmc = 2,2,5,7,8-pentamethylchroman-6-sulfonyl, Trt = trityl) LRLHL pentapeptides **26** were coupled to the liberated carboxylic acids along the scaffold of rod **29**. The reasonably complex product **30** was obtained in good yield. Removal of all protecting groups with HBr/AcOH gave the target rod **4**. Reversed-phase HPLC, MS, and NMR spectra confirmed homogeneity and identity of the final product (see Figures S2 and S3 in the Supporting Information).[37]

Pore **1** was characterized in egg yolk phosphatidylcholine large unilamellar vesicles (EYPC-LUVs) that were loaded with the fluorophore 8-aminonaphtalene-1,3,6-trisulfonate (ANTS) and the quencher *p*-xylenebis(pyridinum)bromide (DPX; EYPC-LUVs⊃ANTS/DPX).[35,42] In this assay, pore activity is detected as fluorogenic efflux of ANTS, DPX, or both. Under these conditions, a Hill coefficient $n = 4.0 \pm 0.2$ was found for pore **1** (Figure 2 A, ●). Moreover, pore **1** could reach full fractional activity $Y_{max} \approx 1.0$ (Figure 2 B, ●). This characteristic ($n > 1$, $Y = 1$) behavior demonstrates endergonic ($n > 1$) self-assembly of tetrameric pores ($n \approx 4$) without competing precipitation from the water at higher concentration ($Y_{max} \approx 1$).[42–44]

These values differed clearly from the previously reported $n = 0.6$ and $Y_{max} \approx 0.4$ for the anchor-free pore **3** (Figure 2, ○).[35,44] This equally characteristic,[42–44] but undesired and more complex ($n = 1$, $Y < 1$) behavior demonstrates exergonic ($n = 1$) self-assembly of pores of unknown stoichiometry ($n = 1$) that occurs already in the water. Exergonic assembly

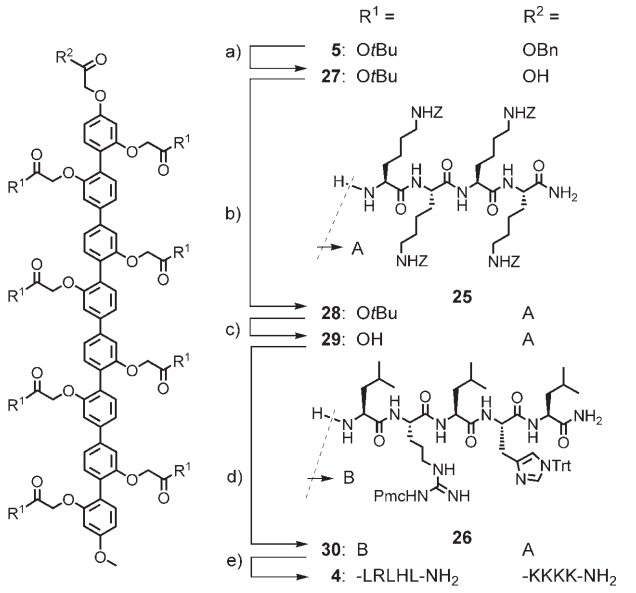

Scheme 2. a) H_2, Pd/C, THF, 1.5 h, RT, yield = 96%; b) HATU, TEA, DMF, 3.5 h, RT, yield = 63%; c) TFA, 2 h, RT, yield = 94%; d) HATU, TEA, DMF, 5.5 h, RT, yield = 75%; e) HBr/AcOH, thioanisole, TFA, pentamethylbenzene, 1.5 h, RT, yield = 68%. Bn = benzyl, DMF = *N*,*N*-dimethylformamide, HATU = *O*-(7-azabenzotriazole-1-yl)-1,1,3,3-tetramethyluronium hexafluorophosphate, TEA = triethylamine.

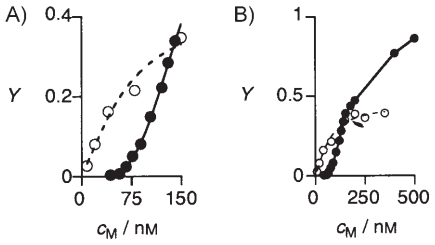

Figure 2. Dependence of the activity Y of pores **1** (●) and **3** (○)[35] in EYPC-LUVs⊃ANTS/DPX on the concentration of the monomeric rods **4**. Data points for **3** (but not for **1**) above 200 nM are not very well reproducible because of competing precipitation from the media.

of pore **3** accounts for both better assembly formation (i.e., higher activity) at low concentrations as well as continuing self-assembly at high concentrations[45] (i.e., precipitation from the water before reaching the membrane, $Y_{max} < 1$); the result is simple saturation behavior.[42–45]

As elaborated in the introduction, the failure to reach full pore activity because of competing precipitation from the water (i.e., $Y_{max} < 1$, Figure 2B, ○) is one of the key obstacles in practical applications of ion channels and pores as drugs, sensors, or catalysts. The clear shift from $n = 0.6$ to $n = 4.0$ confirmed that aqueous anchoring successfully suppressed this exergonic self-assembly in the aqueous phase. Without interference from precipitation at high concentrations, pore **1** was able reach maximal activity (i.e., $Y_{max} \approx 1$, Figure 2B, ●). This access to significant pore activity is, from a practical point of view, one of the most important findings with respect to hydrophilic anchoring.

The biphasic Hill plot of pore **1** confirmed that values measured above the effective pore concentration EC_{50} value (i.e., concentration needed to observe 50% pore activity) reflect the saturation of the assay rather than thermodynamics and cooperativity of pore formation. They should not be used for the determination of Hill coefficients.

In an attempt to further lower the EC_{50} value of pore **1**, the dependence of activity on the concentration of EYPC-LUVs loaded with 5(6)-carboxyfluorescein (EYPC-LUVs⊃CF)[1,25,42] was examined. In this more sensitive assay, pore activity is detected as fluorogenic efflux of CF because local dilution reduces self-quenching. With vesicle dilution, the EC_{50} value of pore **1** in EYPC vesicles decreased to saturation around a minimal $EC_{50,min} = 15$ nM (Figure 3 A, ○). Note that pore concentrations were calculated

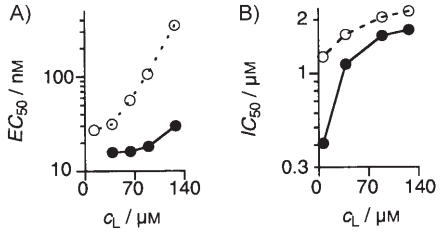

Figure 3. A) The dependence of the EC_{50} value of pore **1** on the concentration of EYPC (●) and EYPC/EYPG 1:1 (○) LUVs⊃CF (given as the total lipid concentration c_L), and B) The dependence of the IC_{50} value of analytes **31** (●) and **32** (○) to block pore **1** on the concentration of EYPC vesicles (given as lipid concentration c_L).

as 25% of the known concentration of monomer **4** ($n = 4$). Considering the endergonic self-assembly of the active tetramer **1**, it is understood that this approximation represents a clear, systematic overestimation.

α-Ketoglutarate hydrazone **31** and pyruvate hydrazone **32** were attractive test analytes to elaborate on the impact of vesicle dilution on stoichiometric binding in sensing applications (Scheme 3). The discrimination of α-ketoglutarate **33** and pyruvate **34** is, for example, of interest for umami sensing with synthetic pores as transducers of signals generated with transaminases. However, all attempts to do so failed so far because of the unavailability of synthetic (or biological) pores that would close or open in response to the recognition of either analyte **33** or analyte **34** at reasonable concentrations. This lack in sensitivity has been overcome with the introduction of amplifiers such as **35**.[1] This hydrazide can react in situ with aldehydes and ketones produced or consumed during enzymatic signal generation and drag them into the pore for detection. Applied to umami sensing, reactive amplification of α-ketoglutarate and pyruvate was found to increase the sensitivity of synthetic pore sensors similar to **2** and **3** by more than four orders of magnitude without interference from amplifier **35** ($IC_{50} = 23$ µM; IC_{50} = blocker concentration required for 50% blockage). The discrimination between α-ketoglutarate hydrazone **31** and pyr-

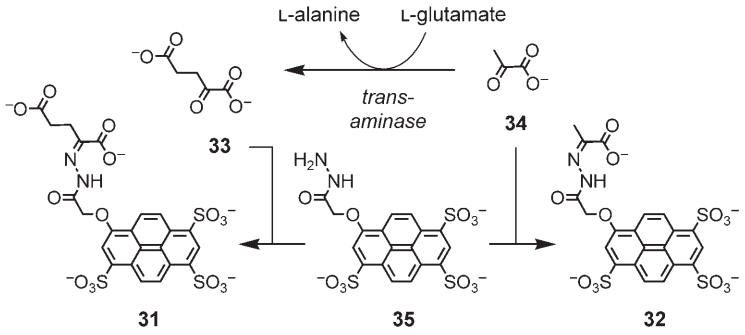

Scheme 3. Sensing scheme for umami sensing with transaminase as the signal generator, hydrazide **35** as the reactive amplifier, and synthetic pores such as **1** as optical transducers.

uvate hydrazone **32** was, however, negligible because of, we speculated, stoichiometric binding.[1]

The detection of amplified α-ketoglutarate **31** and pyruvate **32** by pore **1** under standard conditions occurred with near nanomolar sensitivity (Table 1, entries 1 and 2). As expected for molecular recognition in the zone affected by interference from stoichiometric binding, the discrimination between the two analytes was nearly negligible with $D=1.3$ (where D is the discrimination factor). The IC_{50} values of both hydrazones decreased in response to the reduction of the EC_{50} of pore **1** (Figure 3B and Table 1, entries 3 and 4). These changes in the IC_{50} value resulted in an increase in sensitivity of up to 4.3-fold (Table 1, entries 1 and 3). Also exactly as predicted for reduced interference from stoichiometric binding, this increase in sensitivity coincided with a quite remarkable increase in selectivity. The discrimination factor $D=3.0$ found for the detection of amplified α-ketoglutarate with nanomolar sensitivity ($IC_{50}=400$ nM) is sufficient for sensing applications.[1,36]

Table 1. Blockage data for pore **1**.

Entry	Blocker	Lipid [μM][a]	Pore [nM][b]	IC_{50} [μM][c]	D[d]
1	**31**	124	50	1.7±0.1	1.3
2	**32**	124	50	2.2±0.3	–
3	**31**	6.4	15	0.4±0.1	3.0
4	**32**	6.4	15	1.2±0.2	–
5	ATP	124	50	44.2±3.0	6.1
6	ADP	124	50	267.7±12.6	–
7	ATP	6.4	15	139.5±12.4	4.7
8	ADP	6.4	15	652.1±19.7	–

[a] Approximated from phosphate analysis of final vesicles, assuming a reproducible yield. [b] Approximated as c(pore **1**)=c(monomer **4**)/4 (n=4, Figure 2A); this is a significant overestimate because pore assembly is endergonic. [c] Data ± standard error. [d] Discrimination factor=IC_{50}(ADP)/IC_{50}(ATP) or IC_{50}(**32**)/IC_{50}(**31**).

To confirm the validity of the interpretation of this breakthrough, control dilution experiments without stoichiometric binding were made. ATP/ADP discrimination (ATP=adenosine 5′-triphosphate, ADP=adenosine 5′-diphosphate) provides an ideal example because it is important for the fluorometric detection of many enzymes (e.g., kinases) and the sensing of their substrates.[1,12,13,23,25,36] Under standard conditions, blockage of pore **1** by ATP occurred with $IC_{50}=44.2$ μM and was clearly better than blockage by ADP (Table 1, entries 5 and 6). The high discrimination factor of $D=6.1$ suggested, together with relatively poor IC_{50} values, that nucleotide recognition is not affected by stoichiometric binding. Comparison with results from anchor-free pores obtained under similar conditions demonstrated that ATP/ADP discrimination is not significantly affected by the hydrophilic K_4 anchors. Slightly weaker discrimination factors were reported for anchor-free pores with internal RH dyads as in **1** and **3**[36] (IC_{50}(ATP)=82 μM, $D=3.7$). Slightly better discrimination factors were reported for pores with internal KH dyads (IC_{50}(ATP)=22 μM, $D=10.0$).[1,12,13] Although less-specific and maybe transient interactions with anionic guests are of course likely to occur, this overall excellent similarity with anchor-free pores implied that the K_4 anchors of pore **1** do not contribute constructively to guest recognition.

The IC_{50} value of both nucleotides did not decrease and their discrimination factor D did not increase with a decreasing concentration of pore **1** at a reduced vesicle concentration (Table 1, entries 7 and 8). This control experiment confirmed that the increasing sensitivity and selectivity obtained for the amplifier conjugates **31** and **32** originates from a reduced interference from stoichiometric binding (Table 1, entries 1–4 versus entries 5–8).

The determined increase in sensor sensitivity in response to a reduction of the concentration of pores with increased activity was consistent with the theory of stoichiometric binding. This phenomenon has been studied in detail in the context of enzyme inhibition.[26,27] Assuming one to one binding of the blocker to the pore, one could correlate concentrations of pore [P], blocker [B], and the dissociation constant K_D as is shown in Equation (1).

$$[B]/K_D = i/(100-i) + i[P]/100\ K_D \quad (1),$$

In Equation (1), i is the percent blockage. As the IC_{50} value is the concentration of the blocker that gives rise to 50% pore blockage, the above equation can be simplified as is illustrated in Equation (2).

$$IC_{50/}K_D = 1 + 0.5[P]/K_D \quad (2)$$

Taking this simplification into account, Equation (3) can be derived.

$$IC_{50} = K_D + 0.5[P] \quad (3)$$

Therefore, if the K_D value of the pore–blocker complex is similar or less than the concentration of the pore (K_D=[P]), the IC_{50} values should decrease by lowering the pore concentration. On the other hand, if the K_D value is far greater than the concentration of the pore, the second term in Equation (3) (0.5[P]) becomes negligible and thus the IC_{50}

value would be equal to K_D.

The observed decrease in the IC_{50} value of blockers **31** and **32** by decreasing the concentration of the pore is therefore reasonable if we assume that [P] is similar to or higher than K_D (Table 1, Equation (3)). Note that the concentration of active pores is unknown but certainly less than 25% of the concentration of monomer **4** because of endergonic self-assembly and nonideal partitioning. The K_D value of **32** is thus expected to be well below 15 nM and that of **31** is expected to be even lower because the response to reduced stoichiometric binding is more pronounced ($K_D(\mathbf{31}) < K_D(\mathbf{32}) < [P]$).

In contrast, the increase in the IC_{50} value of ATP and ADP by decreasing the concentration of the pore is not explained by Equation (3). More-complex inhibitory mechanisms may account for these results, including changes in partitioning etc.

Conclusion

In summary, this report introduces hydrophilic anchoring as a promising strategy to increase the sensitivity and the selectivity of synthetic pore sensors. With regard to the activity of the pores as such, the change in the Hill coefficient from $n<1$ to $n=4$ is the most important impact of hydrophilic anchoring. It demonstrates successful suppression of the competing precipitation from the media. The presumably disorganized tetralysine anchors do not interfere with the molecular recognition of anionic blockers by the synthetic pore sensors. The increase in pore activity achieved by hydrophilic anchoring is important because it allowed us to demystify one of the key problems with pore sensors, that is, the origin of the consistent cut-off in sensitivity and selectivity near nanomolar concentrations. Namely, efficiency and selectivity of pore blockers that operate by stoichiometric binding ($K_D = EC_{50}$) are shown to increase in response to a reduction of the effective pore concentration. Controls confirm that this increase does not occur with analytes that are too weak to exhibit stoichiometric binding ($K_D > EC_{50}$).

This breakthrough is significant because it demonstrates that sensitivity and selectivity of pore sensors can be improved by increasing the activity of the pore. The lesson learnt is that, with sufficiently sensitive analyte recognition and amplification accomplished,[1] rational approaches toward "hypersensitive" pore sensors will have to focus on pore–membrane rather than pore–blocker interactions. Examples from biology in support of this conclusion include nisin. This antibiotic peptide may act by targeted pore formation with lipid II at concentrations far below the intrinsic cut-off with other magainin-like natural antibiotics.[46]

This conclusion implied that the introduction of specific lipid–pore interactions would be the key to further increases in sensitivity and selectivity of pore sensors. Incorporation of anionic EYPG into the bilayer so that it could participate in an ion pair with the K_4 anchor of pore **1** was, however, too simplistic an approach toward this objective (Figure 3 A, ○). The determined decreasing activity of pore **1** with increasing surface potential could be explained by preferential ion pairing of lipid phosphates with oligoarginines[47–50] from the barrel rather than oligolysines from the anchor and thus the destruction of the artificial β barrel. Synthetic efforts toward anchor screening in situ and more specifically targeted pore formation for hypersensitive multianalyte sensing are ongoing.

Acknowledgements

We thank A. Pinto and S. Grass for NMR measurements, P. Perrottet and the group of F. Gülaçar for MS measurements, one referee for helpful suggestions, and the Swiss NSF for financial support.

[1] S. Litvinchuk, H. Tanaka, T. Miyatake, D. Pasini, T. Tanaka, G. Bollot, J. Mareda, S. Matile, *Nat. Mater.* **2007**, *6*, 576–580.
[2] T. M. Fyles, *Chem. Soc. Rev.* **2007**, *36*, 335–347.
[3] A. P. Davis, D. N. Sheppard, B. D. Smith, *Chem. Soc. Rev.* **2007**, *36*, 348–357.
[4] J. T. Davis, G. P. Spada, *Chem. Soc. Rev.* **2007**, *36*, 296–313.
[5] R. S. Hector, M. S. Gin, *Supramol. Chem.* **2005**, *17*, 129–134.
[6] U. Koert, L. Al-Momani, J. R. Pfeifer, *Synthesis* **2004**, *8*, 1129–1146.
[7] S. Matile, A. Som, N. Sordé, *Tetrahedron* **2004**, *60*, 6405–6435.
[8] G. W. Gokel, A. Mukhopadhyay, *Chem. Soc. Rev.* **2001**, *30*, 274–286.
[9] P. Scrimin, P. Tecilla, *Curr. Opin. Chem. Biol.* **1999**, *3*, 730–735.
[10] Y. Kobuke, K. Ueda, M. Sokabe, *J. Am. Chem. Soc.* **1992**, *114*, 7618–7622.
[11] J.-H. Fuhrhop, U. Liman, V. Koesling, *J. Am. Chem. Soc.* **1988**, *110*, 6840–6845.
[12] G. Das, S. Matile, *Chem. Eur. J.* **2006**, *12*, 2936–2944.
[13] S. Matile, H. Tanaka, S. Litvinchuk, *Top. Curr. Chem.* **2007**, *277*, 219–250.
[14] *Creative Chemical Sensing Systems. Topics in Current Chemistry* (Ed.: T. Schrader), Springer, Heidelberg, **2007**.
[15] C. Zhang, K. S. Suslick, *J. Agric. Food Chem.* **2007**, *55*, 237–242.
[16] S. Tamaru, S. Kiyonaka, I. Hamachi, *Chem. Eur. J.* **2005**, *11*, 7294–7304.
[17] J. J. Lavigne, E. V. Anslyn, *Angew. Chem.* **2001**, *113*, 3212–3225; *Angew. Chem. Int. Ed.* **2001**, *40*, 3118–3130.
[18] A. Buryak, K. Severin, *J. Am. Chem. Soc.* **2005**, *127*, 3700–3701.
[19] K. Toko, *Biosens. Bioelectron.* **1998**, *13*, 701–709.
[20] C. A. Marquette, A. Degiuli, L. J. Blum, *Biosens. Bioelectron.* **2004**, *19*, 433–439.
[21] L. Campanella, A. Bonanni, E. Finotti, M. Tomassetti, *Biosens. Bioelectron.* **2004**, *19*, 641–651.
[22] A. Hennig, H. Bakirci, W. M. Nau, *Nat. Methods* **2007**, *4*, 629–632.
[23] L. Vial, P. Dumy, *J. Am. Chem. Soc.* **2007**, *129*, 4884–4885.
[24] J. P. Goddard, J.-L. Reymond, *Curr. Opin. Biotechnol.* **2004**, *15*, 314–322.
[25] G. Das, P. Talukdar, S. Matile, *Science* **2002**, *298*, 1600–1602.
[26] B. K. Soichet, *J. Med. Chem.* **2006**, *49*, 7274–7277.
[27] O. H. Straus, A. Goldstein, *J. Gen. Physiol.* **1943**, *26*, 559–585.
[28] P. L. Boudreault, N. Voyer, *Org. Biomol. Chem.* **2007**, *5*, 1459–1465.
[29] J. R. Broughman, L. P. Shank, W. Takeguchi, B. D. Schultz, T. Iwamoto, K. E. Mitchell, J. M. Tomich, *Biochemistry* **2002**, *41*, 7350–7358.
[30] N. Sakai, D. Gerard, S. Matile, *J. Am. Chem. Soc.* **2001**, *123*, 2517–2524.
[31] K. Yamashita, V. Janout, E. Bernard, D. Armstrong, S. L. Regen, *J. Am. Chem. Soc.* **1995**, *117*, 6249–6253.
[32] N. Sakai, J. Mareda, S. Matile, *Acc. Chem. Res.* **2005**, *38*, 79–87.

[33] R. Bhosale, S. Bhosale, G. Bollot, V. Gorteau, M. D. Julliard, S. Litvinchuk, J. Mareda, S. Matile, T. Miyatake, F. Mora, A. Perez-Velasco, N. Sakai, A. L. Sisson, H. Tanaka, D.-H. Tran, *Bull. Chem. Soc. Jpn.* **2007**, *80*, 1044–1057.
[34] D. Ronan, D. Jeannerat, A. Pinto, N. Sakai, S. Matile, *New J. Chem.* **2006**, *30*, 168–176.
[35] P. Talukdar, N. Sakai, N. Sordé, D. Gerard, V. M. F. Cardona, S. Matile, *Bioorg. Med. Chem.* **2004**, *12*, 1325–1336.
[36] N. Sordé, S. Matile, *Biopolymers* **2004**, *76*, 55–65.
[37] See the Supporting Information.
[38] M. Murata, S. Watanabe, Y. Masuda, *J. Org. Chem.* **1997**, *62*, 6458–6459.
[39] N. Sakai, A. L. Sisson, S. Bhosale, N. Banerji, A. Fürstenberg, E. Vauthey, S. Matile, *Org. Biomol. Chem.* **2007**, *5*, 2560–2563.
[40] G. A. Molander, B. Biolatto, *J. Org. Chem.* **2003**, *68*, 4302–4314.
[41] D. Jeannerat, D. Ronan, Y. Baudry, A. Pinto, J.-P. Saulnier, S. Matile, *Helv. Chim. Acta* **2004**, *87*, 2190–2207.
[42] S. Matile, N. Sakai, *The Characterization of Synthetic Ion Channels and Pores. In Analytical Methods in Supramolecular Chemistry*, (Ed.: C. A. Schalley), Wiley, Weinheim, **2007**, 391–418.
[43] S. Bhosale, S. Matile, *Chirality* **2006**, *18*, 849–856.
[44] S. Litvinchuk, G. Bollot, J. Mareda, A. Som, D. Ronan, M. R. Shah, P. Perrottet, N. Sakai, S. Matile, *J. Am. Chem. Soc.* **2004**, *126*, 10067–10075.
[45] G. Das, L. Ouali, M. Adrian, B. Baumeister, K. J. Wilkinson, S. Matile, *Angew. Chem.* **2001**, *113*, 4793–4797; *Angew. Chem. Int. Ed.* **2001**, *40*, 4657–4661.
[46] E. Breukink, B. de Kruijff, *Nat. Rev. Drug Discovery* **2006**, *5*, 321–332.
[47] N. Sakai, S. Matile, *J. Am. Chem. Soc.* **2003**, *125*, 14348–14356.
[48] J. B. Rothbard, T. C. Jessop, R. S. Lewis, B. A. Murray, P. A. Wender, *J. Am. Chem. Soc.* **2004**, *126*, 9506–9507.
[49] T. Takeuchi, M. Kosuge, A. Tadokoro, Y. Sugiura, M. Nishi, M. Kawata, N. Sakai, S. Matile, S. Futaki *ACS Chem. Biol.* **2006**, *1*, 299–303.
[50] D. Schmidt, Q.-X. Jiang, R. MacKinnon, *Nature* **2006**, *444*, 775–779.

Received: September 25, 2007
Revised: November 6, 2007
Published online: December 7, 2007

